Effect of flow conditions on spray cone angle of a two-fluid atomizer

M. Shafaee*, S.A. Banitabaei, M. Ashjaee and V. Esfahanian
Department of Mechanical Engineering
University of Tehran
Tehran 11155-4563 IRAN

Abstract

A visual study is conducted to determine the effect of operating condition on the spray cone angle of a two-fluid atomizer. The liquid (water) jets exit from peripheral inclined orifices and are introduced to a high speed gas (air) stream in the gravitational direction. Using a high speed imaging system, the spray cone angle has been determined for Reynolds numbers ranging from 4×10^4 to 9×10^4 and different Weber numbers up to 140. The results show that the spray cone angle depends on the operating conditions especially in lower values of Reynolds and Weber numbers. Also, an empirical correlation has been obtained to predict the spray cone angle in terms of these two parameters.

Introduction

Two-fluid atomization (also termed as twin-fluid, two-phase, pneumatic and aerodynamic atomization) is one of the liquid disintegration techniques applied to various spraying systems. This type of atomization may be divided into two categories including air-assist and air-blast atomization. In both processes, the bulk liquid to be atomized is first transformed into a jet or sheet at a relatively low velocity and then exposed to a high velocity gas stream [1]. The kinetic energy of the gas flow is used as a source of atomization to shatter the bulk liquid into ligaments that subsequently breakup into droplets [2,3].

Spray angle is one of the important external spray characteristics for evaluating the atomizers performance. Most of the sprays have a conical shape wherein the cone angle is usually defined as the angle between the tangents to the spray envelope at the atomizer exit.

Many practical systems require atomizers that distribute the fuel in the form of a less concentrated and lower penetrated spray. Also, the spray angle of a two-fluid atomizer should be such that it could provide a good mixing between the two fluids which cause the liquid jets to be disintegrated perfectly through the gas stream.

In combustion systems, the value to be selected for the cone angle will depend on the shape of the combustion chamber prior to the air and fuel mixing conditions. Also, the spray angle of a gas turbine combustor has a great effect on its vital parameters including the quality of air and fuel mixing, wall temperature, propulsive power, combustor durability, emission quality and efficiency of energy utilization. Therefore, it will be very important to develop an accurate method for predicting the spray cone angle in such atomizers.

Guo et al. [4] investigated two-phase spraying characteristics of a gas-liquid nozzle used for the humidification of smoke. They found that at the given gas pressure the spray angle will increase gradually with the increasing of liquid phase velocity, while at the given liquid pressure the spray angle decreases with increasing the gas pressure.

Chen and Lefebvre [5] investigated the influence of ambient pressure and liquid physical properties on spray cone angles for a low injection pressure (less than 2 MPa) effervescent atomizer. They observed that for low ambient pressures, the value of spray cone angle increased continuously with an increase in gas to liquid mass ratio (GLR) while at higher pressures it has a maximum value at an intermediate GLR. They explain that the decrease in cone angle at high GLRs is due to the transition of the two-phase flow inside the atomizer exit orifice.

Varde [6] made a liquid fuel spray injected into a gaseous environment in order to investigate the effects of nozzle orifice size and operating conditions on the spray cone angle. The results showed the spray cone angle to depend on the orifice dimensions as well as on the operating conditions. Also, he derived a correlation to predict spray cone angle in terms of Reynolds and Weber numbers.

Laryea and No [7] investigated the cone half-angle of the spray produced by an effervescent diesel injector as a function of GLR, injection and ambient pressures. Their results show that increasing the ambient pressure causes a nonlinear decrease in spray angle followed by an increase that ultimately approaches to an asymptotic value when the pressure reaches 5 MPa. They also suggested an empirical equation to predict the cone angle produced by the tested diesel injector.

* Corresponding author: mshafaee@ut.ac.ir

In general, the spray angle is influenced by nozzle dimensions, liquid properties and the density of the medium into which the liquid is sprayed [8]. In two fluid atomizers, the flow conditions have an important effect on the spray cone angle. Hence, in this study, the spray cone angle of a two-fluid atomizer is investigated at different Reynolds and Weber numbers. The spray angle measurement is based on a visual method using a high speed video camera and image processing technique. An empirical correlation has also been obtained to estimate the spray cone angle in terms of both the Reynolds and Weber numbers.

Experimental Setup and Conditions

Fig. 1 shows a schematic of the experimental setup used in this study comprising three main parts, i.e. the liquid (water) feed line, the compressed gas (air) line and the injector, in addition to the configuration of a high speed video camera system. The first part, the liquid feed line, consists of five elements including a liquid reservoir with a capacity of 1.1 m^3 connected to the main tap water, a stainless steel mesh strainer hampering any possible tiny debris from the liquid flow, a liquid piston pump with a regulating pressure in the range of 0 to 50 bar capable of providing liquid flowrates up to 50 L/min, a needle valve for flowrate adjustment and a rotameter having a measurement range of 0 to 70 L/min with an accuracy of ±1%.

The second part, the compressed air line, is composed of three elements including a pre-charged compressed air reservoir having a capacity of 50 L with a maximum allowable pressure of 140 bar, a mesh strainer followed by an air pressure regulator capable of reducing maximum pressure of 230 bar to a range of 0 to 15 bar. The air flowrates have been calculated based on an air anemometry procedure arranged at the end of a tube which was placed at the outlet of the injector. The appropriate length of the tube provided a fully developed flow for the compressed air at the anemometry section allowing the mean flowrate calculation for different air pressures. The compressed air pressure in addition to the air regulator is also monitored at a location in the vicinity of the injector inlet in order to ensure no air leakage in the air line.

The third part includes an injector, i.e. a two-fluid atomizer, which is connected to the water and compressed air lines using an interface fixture. The fixture is designed to adapt the injector liquid and air entries to the corresponding lines on the setup in addition to mounting the injector in a holder for carrying out subsequent experimental tests.

A schematic of the atomizer and its photographic view are shown in Fig. 2. The compressed air flows through the central part of the atomizer while the liquid feeds through an annular passage mounted on the atomizer periphery. The annular passage ends in six inclined holes which are equally arranged on the atomizer periphery with a sector angle of 60°. Each hole is also placed with an angle of 55° relative to the atomizer central axis without a swirl angle. The liquid lines simultaneously emerging from the holes intercept with the compressed air flow creating the primary atomization zone within the atomizer which, in turn, results in the production of a spray of drops at the atomizer exit. The geometrical parameters of the atomizer, with reference to Fig. 2a, include the liquid inlet diameter d_l=1.6 mm, the atomizer exit diameter d_g=21.5 mm and the air and liquid mixing length L=8 mm.

The visualization system used in this study consists of a high speed digital camera (Mega Speed MS50K) and a side illuminating configuration by using halogen lamp with a power of 1000 Watts. The digital camera is set at a recording rate of 2500 fps with an exposure time of 100 ns capable of recording image files with a resolution of 640×480 pixels. The digital camera simultaneously transmits the captured files to a dedicated PC as well as providing an online display of them. Therefore, the spray angle has been calculated for each flow condition applying an image processing method through a frame by frame analysis followed by a manual verification applied on some random selected pictures as shown in Fig. 3.

Results and Discussion

In the present atomizer, the breakup of liquid jets injected into the air flow, somehow would be similar to the breakup process of a liquid jet by a gas cross flow. But in this atomizer, the transverse interaction between the gas stream and each of the liquid jets and the collision of six liquid jets cause a more complicated atomization phenomena respect to the simple type of the cross flow.

A standard dimensional analysis (Buckingham's p-theorem) shows that all the parameters affect the spray cone angle can be classified into two main groups including geometrical parameters and operating conditions.

Visual investigation shows that by increasing the operational parameters i.e. Reynolds and Weber numbers in a constant geometry, the atomizer passes four different breakup regimes which are Rayleigh, first wind induced, second wind induced and atomization mode. Fig. 4 shows the present atomizer in each of the above mentioned breakup modes.

In the present atomizer, to achieve an atomization mode in each Reynolds number, the kinetic energy of the employed air stream should be able to atomize the liquid jets completely. If the velocity and mass flow rate of the gas jet are insufficient, a non-atomized region would remain in the centre of the spray zone. Fig. 5 shows the

formed dense cores for various Weber numbers. It could be seen that an increase in Weber number, cause the core length to decay.

Since, the spray angle investigations are usually carried out in the atomization mode, thus all the experiments of this study have been performed in appropriate operation conditions, i.e. $Re_l<10^5$ and those Weber numbers that ensure the occurrence of the full atomization mode.

Fig. 6 shows the spray cone angle produced by the two-fluid atomizer as a function of its operating conditions. The curves show that in a constant geometric of atomizer, a similar trend is seen for spray angle variations. In each Weber number, an increase in Reynolds number causes a decrease in spray angle followed by approaching to an asymptotic value for higher Reynolds numbers. Also, increase in the Weber number for a constant value of Reynolds causes the spray cone angle to decrease. The rate of this decrease is considerable at low Weber numbers while for higher values of Weber, the curves will coincide with each other. So, it can be concluded that for $We_g>140$, the spray angle becomes less dependent to Weber number. Consequently, in the present two-fluid atomizer, there are ranges of operating conditions in which the spray angle varies little with Reynolds and Weber numbers. In these ranges, the spray cone angle may only depend to the geometrical parameters of the atomizer.

The following empirical correlation has been developed applying a multiple variable least square regression technique on a set of 36 experimental data to predict the spray cone angle as a function of its operating conditions, i.e. Reynolds and Weber numbers:

$$\theta = -12.56\ln\left(\frac{\mathrm{Re}}{10^4}\right) - 1.55\ln\left(\frac{\mathrm{We}}{10}\right) + 97.72 \qquad 4\times10^4 \le \mathrm{Re} \le 9\times10^4 \quad , \quad \mathrm{We} \le 140. \tag{1}$$

It should be noted that the image taking and processing of each flow condition has been repeated 5 times to assure the repeatability of the results gained for the cone angle. An error analysis indicates that Eq. (1) is applicable over the entire range defined for Reynolds and Weber numbers with a maximum error of 6.4%. Spray cone angles calculated using the above correlation are plotted against the measured values in Fig. 7. In most cases the correlation is seen to predict the spray cone angle fairly accurately.

Nomenclature

d_g	atomizer exit diameter [mm]
d_l	liquid port diameter [mm]
L	length of gas-liquid mixing chamber [mm]
Re	Reynolds number
We	Weber number

Subscripts

g	gas
l	liquid

References

[1] Lefebvre, A.H., *Atomization and Sprays* 2:101-119 (1992).
[2] Marmottant, P., and Villermaux, E., *Journal of Fluid Mechanics* 498:73-111 (2004).
[3] Ng, C.L., Sankarakrishnan, R., and Sallam, K.A., *International Journal of Multiphase Flow* 34:241-259 (2008).
[4] Guo, L.J., Li, G.J., Chen, B., Chen, X.J., Papailiou, D.D., and Panidis, Th., *Experimental Thermal and Fluid Science* 26:715-722 (2002).
[5] Chen, S.K., and Lefebvre, A.H., *Atomization and Sprays* 4:291-301 (1994).
[6] Varde, K.S., *Canadian Journal of Chemical Engineering* 63:183-187 (1985).
[7] Laryea, G.N., and No, S.Y., *Journal of Electrostatics* 60:37-47 (2004).
[8] Lefebvre, A.H., *Atomization and Sprays*, Hemisphere, 1989, pp. 281-282.

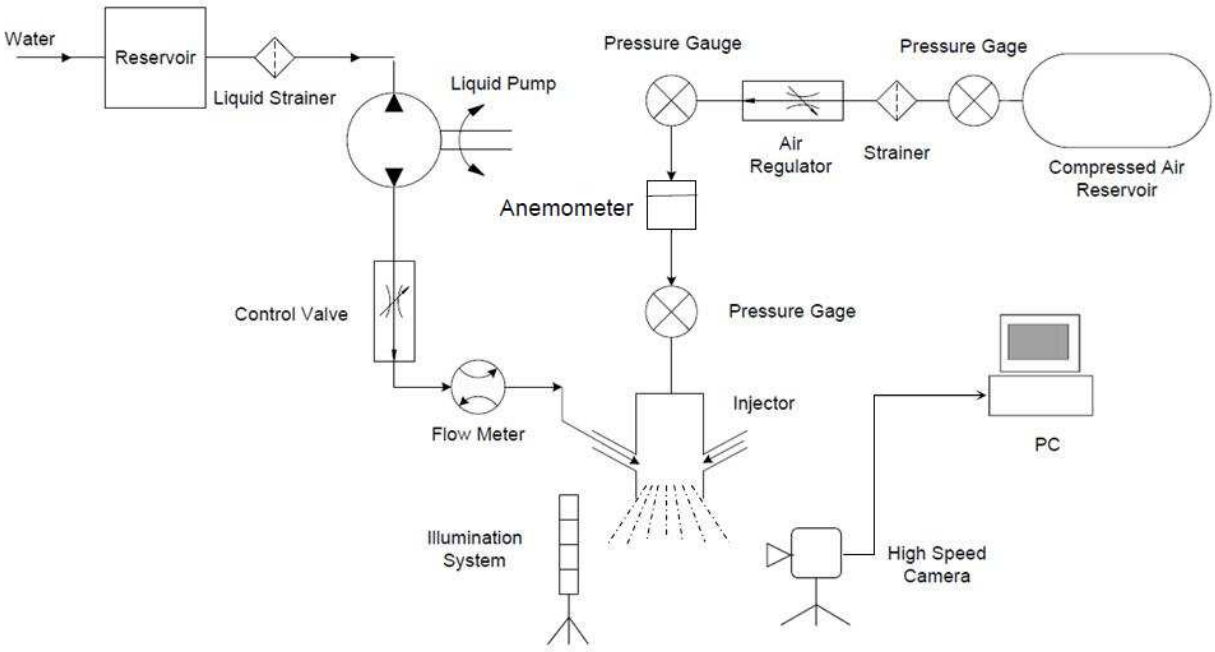

Figure 1. Schematic view of the experimental setup

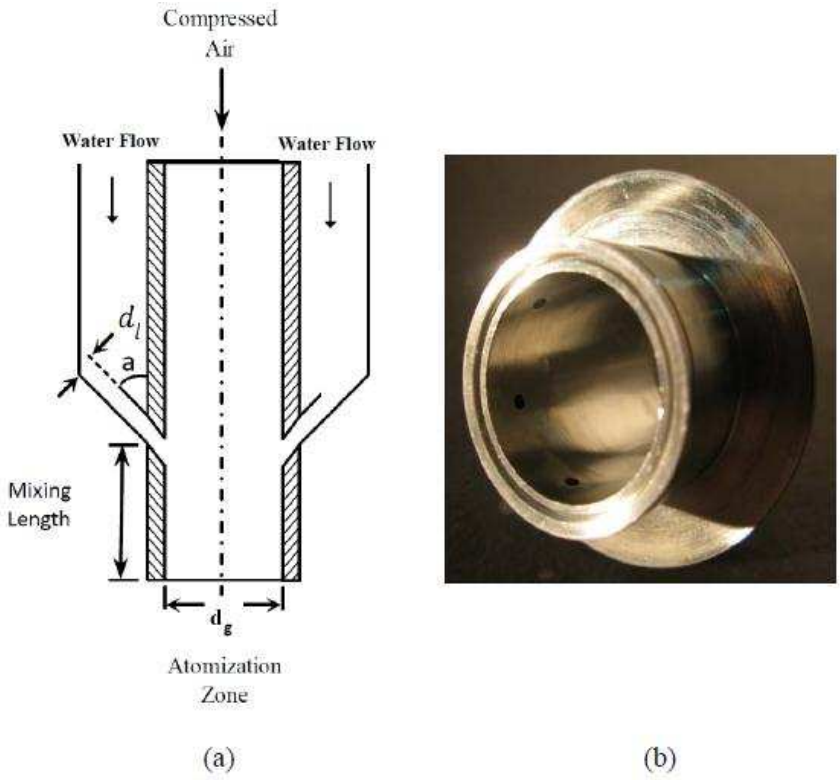

Figure 2. The two-fluid atomizer used in this study, (a) a schematic, (b) a photographic view

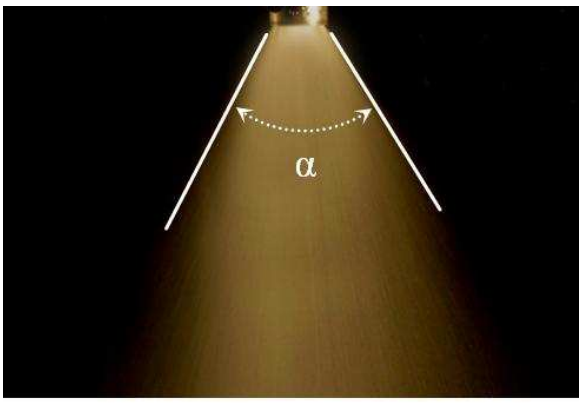

Figure 3. Manual verification of determined spray cone angle

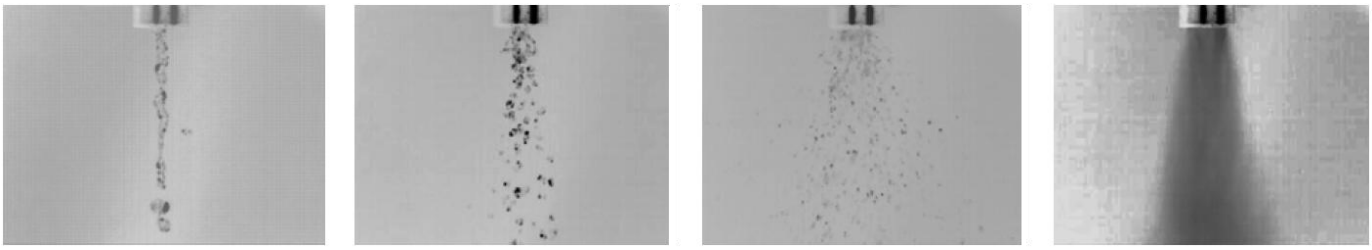

Figure 4. Different breakup modes based on Weber increment (Re_l=1650)

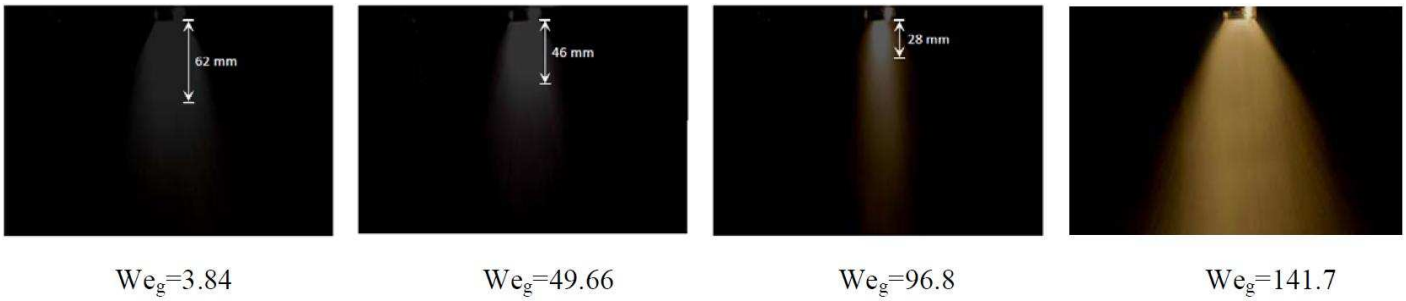

Figure 5. Variations of the dense core length in different Weber numbers ($Re_l=1.2\times10^5$)

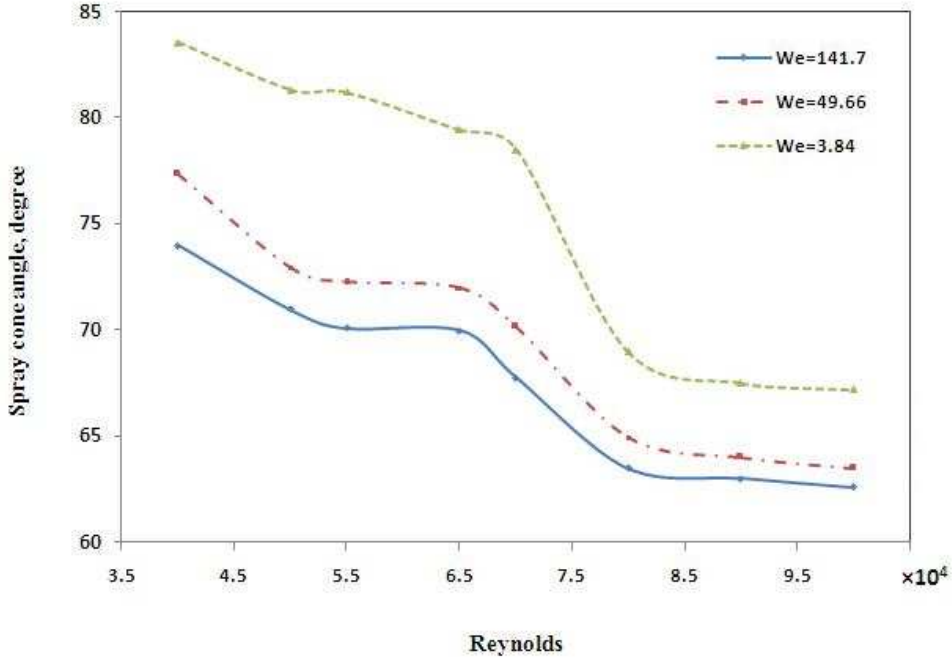

Figure 6. Spray angle variations against Reynolds in different Weber numbers

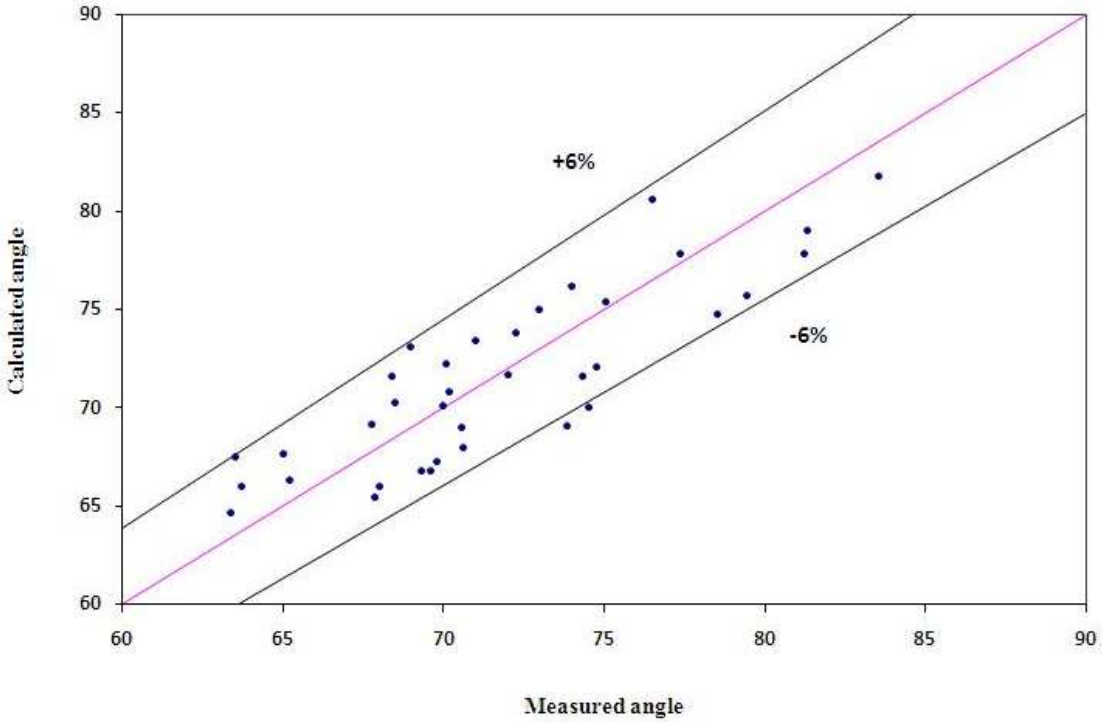

Figure 7. Correlation accuracy plot